

Communication

Fabrication of Two-Layered Aluminum Foam with Closed-Cell and Open-Cell Structures and Shaping of Closed-Cell Layer by Press Forming Immediately after Foaming

Yoshihiko Hangai *, Mizuki Ando, Masataka Ohashi and Kenji Amagai

Graduate School of Science and Technology, Gunma University, Kiryu 376-8515, Japan;
†15302006@gunma-u.ac.jp (M.A.); †15302020@gunma-u.ac.jp (M.O.); amagai@gunma-u.ac.jp (K.A.)

* Correspondence: hanhan@gunma-u.ac.jp; Tel.: +81-277-30-1554

Abstract: Two-layered aluminum foam consisting of both closed and open cells is expected to improve the functionality of aluminum foam, because the cells have different morphologies and characteristics. In this study, press forming of the closed-cell layer of the two-layered aluminum foam immediately after foaming was performed to shape the closed-cell layer. By measuring the temperatures of the two layers during foaming, we found that it is necessary to use aluminum alloy with a higher melting point for the open-cell layer than that for the closed-cell layer to foam the closed-cell layer. In the press forming experiments, the closed-cell layer could be shaped by press forming while the shape of the open-cell layer was maintained.

Keywords: functionally graded materials; cellular materials; sintering; press forming



Citation: Hangai, Y.; Ando, M.; Ohashi, M.; Amagai, K. Fabrication of Two-Layered Aluminum Foam with Closed-Cell and Open-Cell Structures and Shaping of Closed-Cell Layer by Press Forming Immediately after Foaming. *Metals* **2021**, *11*, 140. <https://doi.org/10.3390/met11010140>

Received: 29 December 2020

Accepted: 11 January 2021

Published: 12 January 2021

Publisher's Note: MDPI stays neutral with regard to jurisdictional claims in published maps and institutional affiliations.



Copyright: © 2021 by the authors. Licensee MDPI, Basel, Switzerland. This article is an open access article distributed under the terms and conditions of the Creative Commons Attribution (CC BY) license (<https://creativecommons.org/licenses/by/4.0/>).

1. Introduction

Multifunctional materials are expected in several industrial fields, such as transportation equipment and construction materials. Aluminum foam has the potential to satisfy those demands [1,2]. In aluminum foam, many pores exist in the aluminum matrix. These pores are divided into closed-cell pores and open-cell pores [3]. In closed-cell aluminum foam, pores are separated from each other by aluminum cell walls. It exhibits good energy absorption and thermal insulation properties with an excellent light weight that allows it to float on water. Baumgartner et al. [4] and Duarte and Banhart [5] demonstrated the precursor foaming process for fabricating closed-cell aluminum foam. In this process, a blowing agent powder is mixed in the aluminum matrix to fabricate a foamable precursor. The precursor expands during heat treatment owing to the gases released by the decomposition of the blowing agent, resulting in closed-cell aluminum foam. The advantages and recent progress of this process were described in [6,7]. In open-cell aluminum foam, pores are connected with each other. It exhibits good sound insulation and heat dissipation (heat exchange) properties with an excellent light weight. Zhao and Sun [8] demonstrated the sintering and dissolution process (SDP), which is categorized as a space holder process, for fabricating open-cell aluminum foam. In the SDP, a sodium chloride (NaCl) powder is mixed with an aluminum powder. Then the aluminum powder is sintered before being placed into water to dissolve the NaCl in the sample. The advantages and recent progress of this process were described in [9,10].

Recently, two-layered aluminum foam consisting of both closed and open cells has been fabricated [11]. Because the closed-cell aluminum foam and open-cell aluminum foam have different morphologies and characteristics, it is expected that aluminum foam with different pore structures will have improved functionality. In the investigation of the compression properties of the two-layered aluminum foam [12], the closed-cell layer was first freely foamed, then the foamed layer was machined to form shaped specimens for compression tests. NaCl in the sample strengthened the open-cell layer so that it withstood

the machining process. Thereafter, NaCl was dissolved in water. The shaping of aluminum foam is indispensable for the manufacturing of aluminum foam parts. The machining process is a fast process for fabricating the required shape. However, there is the concern that the surface pores might collapse and the machined aluminum chips will fill the pores during the machining process [13,14]. In addition, the thin dense layer generated at the surface of the aluminum foam, called skin, was also removed by the machining process. The surface skin is expected to improve the strength of aluminum foam, such as in an aluminum foam core sandwich [15,16]. Therefore, it is desirable to retain the surface skin during the shaping of aluminum foam.

Recently, the technique of press forming of softened aluminum foam during or immediately after the foaming of the precursor was developed [17,18]. In the press forming process, first, the precursor was heat-treated using halogen lamps. When the precursor temperature exceeded the liquidus temperature of the aluminum matrix, the precursor vigorously foamed [5]. After the precursor was sufficiently foamed, press forming was conducted before the temperature decreased to below the liquidus temperature. In this forming process, the surface skin remained.

In this study, the press forming of the closed-cell layer of the two-layered aluminum foam was performed. However, there was concern that the open-cell layer might collapse during foaming and press forming processes upon exceeding the melting point of the aluminum matrix of the open-cell layer. Therefore, the aim of this study is to observe whether the open-cell layer reached the melting point of the aluminum matrix by the temperature measurement of both layers during the foaming process. Two types of sample were subjected to the temperature measurement: one in which a different type of aluminum matrix was used for the two layers and another in which the same type of aluminum matrix was used for both layers. Thereafter, the press forming of the closed-cell layer using various shaped dies was attempted.

2. Materials and Methods

2.1. Fabrication Procedure for Sintered Sample

Figure 1a–c shows the fabrication procedure for the sintered sample consisting of an upper precursor layer and lower SDP layer. As shown in Figure 1a, Al-Si-Mg alloy (AC4CH, ~25 μm , Toyo Aluminium K.K., Osaka, Japan), titanium hydride (TiH_2 , <45 μm , Kojundo Chemical Lab. Co., Ltd., Sakado, Japan) as a blowing agent, and alumina (Al_2O_3 , ~1 μm , Kojundo Chemical Lab. Co., Ltd., Sakado, Japan) as a stabilization agent powder were mixed as Mixture I. The amounts of TiH_2 and Al_2O_3 were 1 wt.% and 5 wt.%, respectively, with respect to the weight of AC4CH. Pure aluminum (pAl, ~20 μm , Kojundo Chemical Lab. Co., Ltd., Sakado, Japan) and sodium chloride (NaCl, sieved to 355–425 μm , The Salt Industry Center of Japan, Odawara, Japan) as a space holder powder were mixed as Mixture II at a volume fraction of 3 to 7. Next, as shown in Figure 1b, Mixtures I and II were introduced into the carbon die layer by layer. Then the layered mixtures were sintered by spark plasma sintering (SPS). The holding temperature, pressure, and time during SPS were 520 $^\circ\text{C}$, 50 MPa, and 5 min, in accordance with [19]. Figure 1c shows AC4CH/pAl as a sintered sample with a diameter of 20 mm and height of 20 mm. In addition, another sintered sample with the aluminum matrix of the lower SDP layer changed from pAl to AC4CH (AC4CH/AC4CH sample) was fabricated for comparison.

2.2. Temperature Measurement Procedure during Foaming

Figure 1d shows the foaming procedure of the upper-layer AC4CH precursor of the sintered sample. The sintered sample was placed on a ceramic honeycomb. The temperature at the center of each layer during the foaming process was measured with a K-type thermocouple. The thermocouples were put into holes previously drilled into each layer. Four 2 kW halogen lamps were used for foaming the upper precursor in accordance with [20]. The current and voltage applied to each lamp were 9 A and 180 V. The foaming behavior was recorded with a video camera.

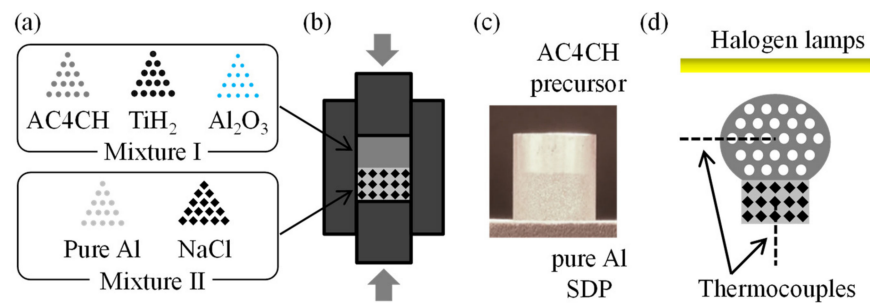


Figure 1. Fabrication of two-layered (AC4CH/pAl) Al foam. (a) Base powders. (b) Sintering. (c) As-sintered sample consisting of an upper precursor layer and lower sintering and dissolution (SDP) layer. (d) Foaming.

2.3. Press Forming Procedure

The AC4CH/pAl sample was subjected to press forming of the foamed upper-layer precursor, as shown in Figure 2. The temperature was not measured in this experiment because it was considered that thermocouples would disturb the forming. Figure 2a shows the setup of foaming and press forming. A robot arm, Single Axis Robots RS2 (MISUMI Group Inc., Tokyo, Japan), was used for press forming. Two stainless-steel bars were attached to the robot arm. Then, the press forming die was attached to the two stainless-steel bars. The lower pAl layer was covered with a copper plate to prevent the press-formed AC4CH foam from covering the surface of the pAl layer. After aluminum foam was sufficiently foamed, as shown in Figure 2b, the die attached to the robot arm was inserted between the lamps and foamed sample. Then, the lamps were turned off and the die was moved downwards at $v = 100$ mm/s for press forming of the upper foamed layer. The aluminum foam was cooled in air with the die remaining in contact with the surface of the formed aluminum foam, as shown in Figure 2c. Then the die was moved upwards after the aluminum foam was sufficiently solidified. The foaming and forming behaviors were recorded with a video camera.

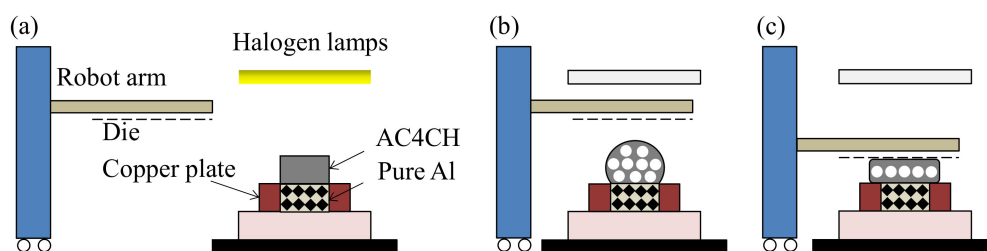


Figure 2. Schematic illustration of foaming and press forming. (a) Start of heating. (b) Insertion of forming die after foaming and end of heating. (c) Press forming.

3. Results

3.1. Temperature Measurement during Foaming

Figure 3 shows the foaming behavior of the AC4CH/pAl sintered sample and corresponding foaming time t –temperature T relationships. $t = 0$ was defined as the start of the heat treatment. (a)–(c) in Figure 3d, respectively, correspond to Figure 3a–c. Figure 3a shows the sample at the beginning of heat treatment. Figure 3b shows the sample when the upper AC4CH layer was gradually foaming. Observations indicated that the AC4CH layer gradually foamed right after the temperature of the AC4CH layer exceeded the solidus temperature of AC4CH (555 °C [21]). Figure 3c shows the sample when the AC4CH layer was sufficiently foamed when the temperature of the AC4CH layer reached the liquidus temperature of AC4CH (610 °C [21]). At this point, although the lower pAl layer also

indicated a temperature similar to that of the AC4CH layer, it did not reach the melting point of pAl (660 °C [21]). In addition, it is shown in Figure 3c that no deformation or collapse of the pAl layer can be observed.

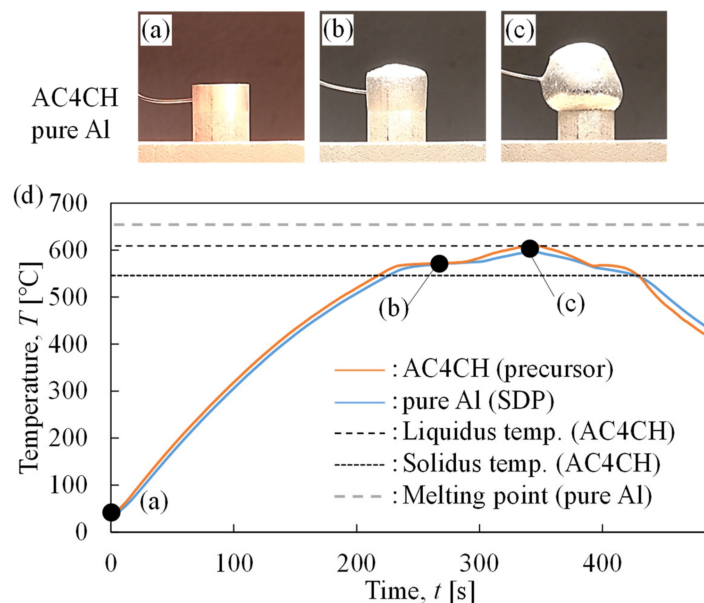


Figure 3. Foaming behavior and corresponding temperature history of AC4CH/pAl. (a) Beginning of heat treatment. (b) Gradual foaming of upper AC4CH layer. (c) Sufficient foaming of upper AC4CH layer. (d) Foaming time t -temperature T relationships.

Figure 4 shows the foaming behavior of the AC4CH/AC4CH sintered sample and corresponding foaming time t -temperature T relationships. Figure 4a shows the sample at the beginning of the heat treatment of the sample. Figure 4b shows the sample when the upper AC4CH layer was gradually foaming. Figure 4c shows the sample when the upper AC4CH was sufficiently foamed. This foaming behavior was similar to the foaming of the AC4CH/pAl sample except that a slight deformation of and crack generation in the lower layer were observed. Note that the temperature of the lower layer was slightly lower than that of the upper layer, which was different from the situation of the AC4CH/pAl sample shown in Figure 3. This is probably due to the difference in the thermal conductivities of pAl (238 W/m·°C [21]) and AC4CH (159 W/m·°C [21]). However, the temperature of the lower SDP layer exceeded the solidus temperature of AC4CH when the upper layer was sufficiently foamed. That is, it is necessary to use aluminum alloy with a higher melting point for the SDP layer than that for the precursor layer to fabricate aluminum foam with both closed-cell and open-cell pore structures by the foaming process.

3.2. Press Forming of Closed-Cell Layer

Figure 5 shows the foaming and press forming behavior of the upper AC4CH layer of the AC4CH/pAl sample. Figure 5a shows the initial precursor before foaming. Note that the lower pAl layer was covered with a copper plate. When the AC4CH layer was sufficiently foamed (Figure 5b), press forming was conducted, as shown in Figure 5c. A commercially pure A1050 aluminum plate of 3 mm thickness with steel mesh on the surface was used as the press forming die. As shown in Figure 5d, a flat AC4CH foam layer was obtained by press forming, with the lower layer maintaining its shape.

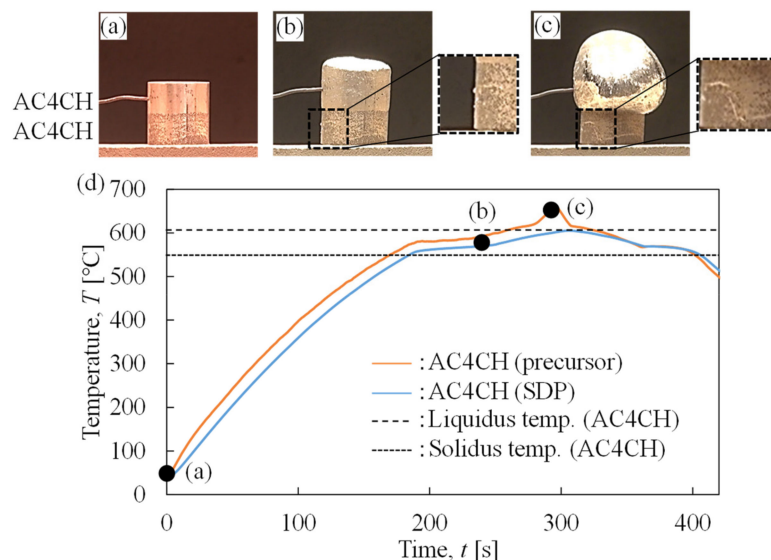


Figure 4. Foaming behavior and corresponding temperature history of AC4CH/AC4CH. (a) Beginning of heat treatment. (b) Gradual foaming of upper AC4CH layer. (c) Sufficient foaming of upper AC4CH layer. (d) Foaming time t –temperature T relationships.

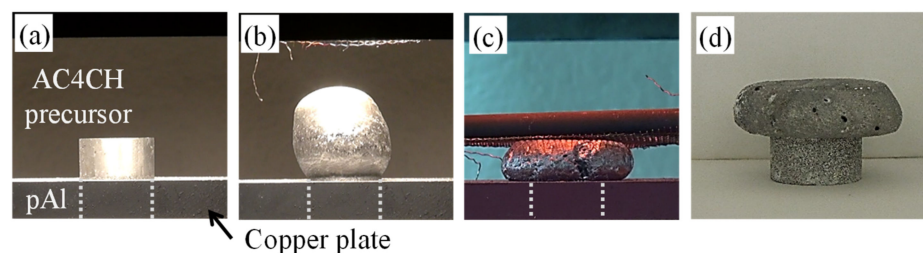


Figure 5. Foaming and press forming behavior of AC4CH/pAl sample when using flat die. (a) Before foaming. (b) Foamed. (c) Press formed. (d) Flattened AC4CH layer sample.

Figure 6 shows another AC4CH/pAl two-layered aluminum foam press formed using various dies, as shown in Figure 6a,b. It is seen that a triangular closed-cell layer (Figure 6c) and waveform surface closed-cell layer (Figure 6d) can be obtained, with the lower layer maintaining its shape.

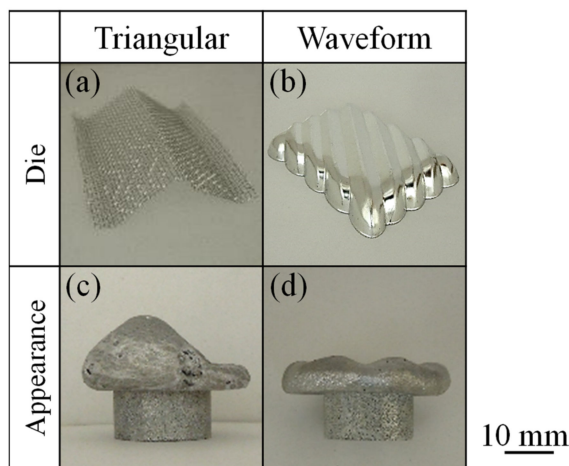


Figure 6. Press formed dies and obtained AC4CH/pAl samples. (a) Triangular die. (b) Waveform surface die. (c) Triangular AC4CH/pAl sample. (d) Waveform surface AC4CH/pAl sample.

4. Conclusions

In this study, press forming of the closed-cell layer of two-layered aluminum foam consisting of a closed-cell layer and an open-cell layer was performed. The temperature of both layers was measured during foaming. The experimental results led to the following conclusions.

(1) It is necessary to use aluminum alloy with a higher melting point for the open-cell layer than that for the closed-cell layer to successfully foam the closed-cell layer while maintaining the shape of the open-cell layer.

(2) The closed-cell layer can be shaped by press forming with the open-cell layer maintaining its shape.

(3) Closed-cell layers of various shapes can be obtained by press forming using variously shaped dies.

Author Contributions: Conceptualization, Y.H. and K.A.; investigation, M.A. and M.O.; writing—original draft preparation, Y.H.; writing—review and editing, Y.H. and K.A. All authors have read and agreed to the published version of the manuscript.

Funding: This research was funded by the Light Metal Education Foundation and JST-Mirai Program, grant number JPMJMI19E5, Japan.

Institutional Review Board Statement: Not applicable.

Informed Consent Statement: Not applicable.

Data Availability Statement: The data presented in this study are available on request from the corresponding author.

Acknowledgments: The authors are grateful to Toyo Aluminium K.K. of Japan for providing the AC4CH alloy powder, and The Salt Industry Center of Japan for providing the NaCl powder.

Conflicts of Interest: The authors declare no conflict of interest.

References

1. Banhart, J. Manufacture, characterisation and application of cellular metals and metal foams. *Prog. Mater. Sci.* **2001**, *46*, 559–632. [[CrossRef](#)]
2. García-Moreno, F. Commercial Applications of Metal Foams: Their Properties and Production. *Materials* **2016**, *9*, 85. [[CrossRef](#)]
3. Gibson, L.J. Mechanical behavior of metallic foams. *Annu. Rev. Mater. Sci.* **2000**, *30*, 191–227. [[CrossRef](#)]
4. Baumgartner, F.; Duarte, I.; Banhart, J. Industrialization of powder compact foaming process. *Adv. Eng. Mater.* **2000**, *2*, 168–174. [[CrossRef](#)]
5. Duarte, I.; Banhart, J. A study of aluminium foam formation—Kinetics and microstructure. *Acta Mater.* **2000**, *48*, 2349–2362. [[CrossRef](#)]
6. Duarte, I.; Oliveira, M.; Garcia-Moreno, F.; Mukherjee, M.; Banhart, J. Foaming of AA 6061 using multiple pieces of foamable precursor. *Colloids Surf. A Physicochem. Eng. Asp.* **2013**, *438*, 47–55. [[CrossRef](#)]
7. Duarte, I.; Vesenjak, M.; Vide, M.J. Automated Continuous Production Line of Parts Made of Metallic Foams. *Metals* **2019**, *9*, 531. [[CrossRef](#)]
8. Zhao, Y.Y.; Sun, D.X. A novel sintering-dissolution process for manufacturing Al foams. *Scr. Mater.* **2001**, *44*, 105–110. [[CrossRef](#)]
9. Stanev, L.; Kolev, M.; Drenchev, B.; Drenchev, L. Open-Cell Metallic Porous Materials Obtained through Space Holders-Part I: Production Methods. A Review. *J. Manuf. Sci. Eng. Trans. ASME* **2017**, *139*. [[CrossRef](#)]
10. Stanev, L.; Kolev, M.; Drenchev, B.; Drenchev, L. Open-Cell Metallic Porous Materials Obtained Through Space Holders-Part II: Structure and Properties. A Review. *J. Manuf. Sci. Eng. Trans. ASME* **2017**, *139*. [[CrossRef](#)]
11. Hangai, Y.; Ikeda, H.; Amagai, K.; Suzuki, R.; Matsubara, M.; Yoshikawa, N. Fabrication of two-layered aluminum foam having layers with closed-cell and open-cell pores. *Metall. Mater. Trans. A* **2018**, *49*, 4452–4455. [[CrossRef](#)]
12. Hangai, Y.; Ando, M.; Ohashi, M.; Amagai, K.; Suzuki, R.; Matsubara, M.; Yoshikawa, N. Compressive properties of two-layered aluminum foams with closed-cell and open-cell structures. *Mater. Today Commun.* **2020**, *24*. [[CrossRef](#)]
13. Matsumoto, R.; Tsuruoka, H.; Otsu, M.; Utsunomiya, H. Fabrication of skin layer on aluminum foam surface by friction stir incremental forming and its mechanical properties. *J. Mater. Process. Technol.* **2015**, *218*, 23–31. [[CrossRef](#)]
14. Matsumoto, R.; Mori, S.; Otsu, M.; Utsunomiya, H. Formation of skin surface layer on aluminum foam by friction stir powder incremental forming. *Int. J. Adv. Manuf. Technol.* **2018**, *99*, 1853–1861. [[CrossRef](#)]
15. Banhart, J.; Seeliger, H.W. Aluminium Foam Sandwich Panels: Manufacture, Metallurgy and Applications. *Adv. Eng. Mater.* **2008**, *10*, 793–802. [[CrossRef](#)]

16. Banhart, J.; Seeliger, H.W. Recent Trends in Aluminum Foam Sandwich Technology. *Adv. Eng. Mater.* **2012**, *14*, 1082–1087. [[CrossRef](#)]
17. Hangai, Y.; Ohashi, M.; Nagahiro, R.; Amagai, K.; Utsunomiya, T.; Yoshikawa, N. Press forming of aluminum foam during foaming of precursor. *Mater. Trans.* **2019**, *60*, 2464–2469. [[CrossRef](#)]
18. Hangai, Y.; Kawato, D.; Ando, M.; Ohashi, M.; Morisada, Y.; Ogura, T.; Fujii, H.; Nagahiro, R.; Amagai, K.; Utsunomiya, T.; et al. Nondestructive observation of pores during press forming of aluminum foam by X-ray radiography. *Mater. Charact.* **2020**, *170*, 110631. [[CrossRef](#)]
19. Hangai, Y.; Morita, T.; Utsunomiya, T. Functionally graded aluminum foam consisting of dissimilar aluminum alloys fabricated by sintering and dissolution process. *Mater. Sci. Eng. A* **2017**, *696*, 544–551. [[CrossRef](#)]
20. Hangai, Y.; Amagai, K.; Omachi, K.; Tsurumi, N.; Utsunomiya, T.; Yoshikawa, N. Forming of aluminum foam using steel mesh as die during foaming of precursor by optical heating. *Opt. Laser Technol.* **2018**, *108*, 496–501. [[CrossRef](#)]
21. The Japan Institute of Light Metals. *Structures and Properties of Aluminum*; The Japan Institute of Light Metals: Tokyo, Japan, 1991.